Fluorescent Nanosensors for Monitoring Ions in Biosamples

T. Doussineau, A. Schulz, S. Trupp, B. Bussemer, S. Körsten, P. Cywinski, A. Moro, A. Lapresta-Fernandez and G. J. Mohr
Institute of Physical Chemistry, Friedrich-Schiller University Jena
Lessingstrasse 10, D-07743 Jena
E-Mail: gerhard.mohr@uni-jena.de

1. Introduction

Fluorescent nanoparticles have recently found increasing interest in medical and biological research. Significant improvements have already been achieved for the detection of ions and biomolecules in living cells, tissues and microorganisms in comparison to conventional fluorescent probes. In a general point of view, dyes embedded in a polymeric matrix show a better photostability thanks to the spatial constraint of the dye molecule together with the limited access of dioxygen within the matrix. Additionally, the system dye@matrix exhibits a higher brightness due to the high concentration of the emittiing molecules within a reduced space and this without the limitations observed in solution like the aggregation phenomenon. In biological medium, the embedding of the dye reduces its toxicity and non-specific interactions with biomolecules like proteins that can cause mis-interpretation in the changes of the optical signal. Finally, it is possible to immobilise not only indicator dyes but also inert reference dyes in the particles. This allows ratiometric measurements for reliable and continuous analyte monitoring (see Fig1).

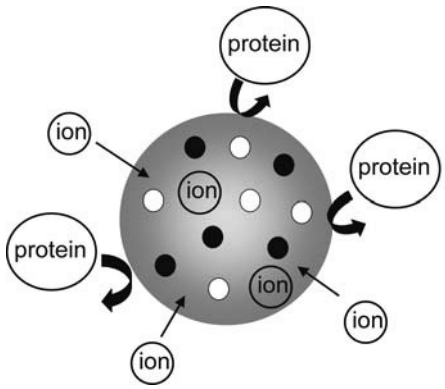

Figure 1. Schematic drawing of a nanosensor and its interaction with ions and proteins. Ions can freely diffuse into the matrix of the nanoparticle where they interact with the indicator dye (black circles, white circles represent the reference dye molecules), whereas bigger proteins cannot enter the matrix.

Based on these principles, we report here results on the development of nanosensors for H^+ and Cl^- that constitute promising tools for bioanalysis. Advantages and limitations of polymer matrices will be discussed.

2. pH-nanosensor [1]

In the field of biology and medicine, sensors able to monitor pH in real-time are highly demanded for the general understanding of biological processes and for biomedical diagnosis. Indeed intra- and extracellular proton concentration is a relevant biomarker of the cell activity and allows, as an example, the characterization of cancer cells. Various research groups have recently developed procedures yielding spherical, small and mono-disperse dye-doped silica nano-particles capable for non-invasive insertion into living cells. [2] Single pH-sensitive dye or two-dye nano-sensors were described, the latter allowing quantitative real-time pH-monitoring based on the principle of ratiometric measurements.

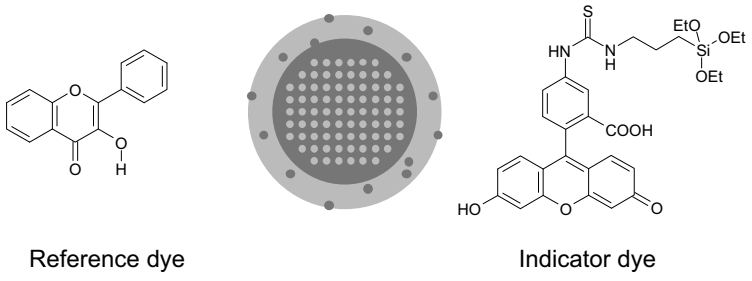

Figure 2. Structures of the dyes and scheme of the nanosensor. Circles represent either the reference dye molecules (dispersed in the ordered porosity of the zeolite *beta* core) or the pH-sensitive dye molecules (randomly dispersed in the amorphous silica shell).

The nanosensor described here is compartmented in a core-shell architecture. This will provide a better accessibility of the sensing dye to the analyte while it will avoid Förster resonance energy transfer to occur between the two dyes. The zeolite *beta* core contains the 3-hydroxyflavone chromophore (3HF, reference dye) while the shell is made of amorphous silica encapsulating pH-sensitive fluorescein (see Fig2). Zeolite *beta* colloids are prepared in hydrothermal conditions using a structure-directing agent which is then removed from the structural microporosity by calcination. The 3HF molecules are encapsulated by simple impregnation of the dye in the liquid phase. Thanks to strong host-guest interactions, chromophores are firmly anchored within the matrix. The subsequent sensing silica shell is formed through a seed-growing approach by adding silica precursor together with the silylated fluorescein.

In a morphological point of view, the resulting nanosensor is spherical in shape and an increase in size after the coating of the sensing shell is observed in transmission electron microscopy (see Fig3a) as well as in dynamic light scattering (see Fig3b). Structurally, evidence of the coating of the sensing silica shell is visible on the wide-angle X-ray diffractogram with the appearance of a broad diffraction peak centered at 2θ=24° corresponding to amorphous silica (see Fig3c).

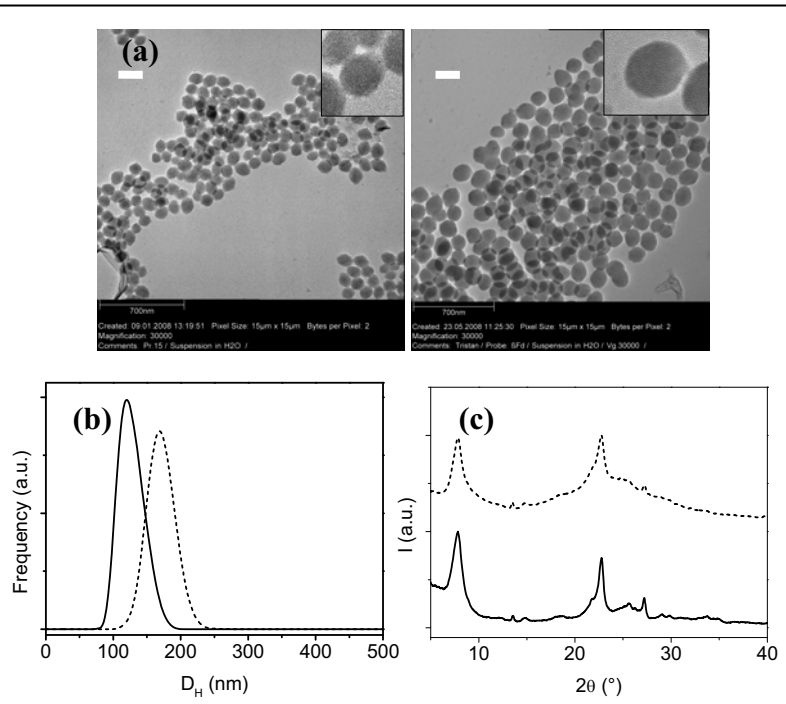

Figure 3. (a) TEM images of the reference core (left) and the resulting nanosensor after coating of the sensing layer (right) ; (b) Corresponding DLS size distribution profile ; (c) Corresponding XRD patterns.

Investigations on the pH sensitivity of the resulting nanosensor were conducted using steady-state fluorescence spectrometry. The fluorescence intensity of the 3HF reference dye embedded within the zeolite *beta* core does not change significantly by modifying the pH of the nanoparticles dispersion in the pH range 5-8. However the fluorescence intensity of fluorescein molecules embedded in the amorphous silica shell is, as expected, strongly affected by changing pH (see Fig4a). Changes in fluorescence intensity of the pH indicator in the different pH buffered solutions are observed within few seconds indicating an easy accessibility of the embedded dye to H^+ through the pores of the silica shell. The ratio between sensing and reference dye against pH can be fitted by a sigmoidal curve from which an apparent pK_a of 6.4 was calculated similar to the one in solution (see Fig4b). Furthermore, in order to investigate the stability in response calibration, particles were dispersed in aqueous buffered solutions with increased

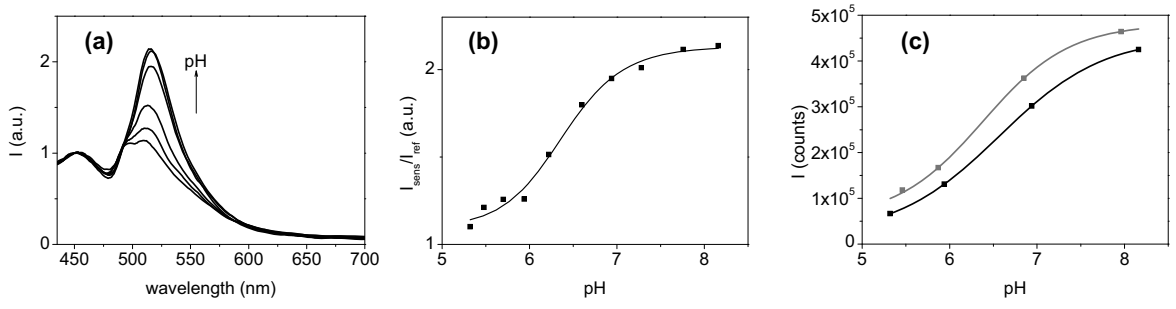

Figure 4. (a) Fluorescence spectra of pH-nanosensors suspended into buffers of different pH, λ_{ex} = 400 nm ; (b) Point by point graphic of the fluorescence intensity ratio between indicator dye (λ_{em} = 515 nm) and reference dye (λ_{em} = 445 nm) against pH and its sigmoidal fit ; (c) Changes in the intensity of pH-nanosensors in phosphate buffered solutions (black points) and in phosphate buffered saline (0.12 M) solutions containing 1% w/w bovine serum albumin (gray points) and the corresponding sigmoidal fit curves.

ionic strength (potassium chloride 0.12 M) together with the addition of a protein (bovine serum albumin, Aldrich, 1% w/w). Both the ionic strength as well as addition of protein to the nanoparticles suspension did not significantly affect the fluorescence intensity of the sensing dye (see Fig4c).

3. Chloride-nanosensor [3]

Among the anions, chloride plays a central role in many biological processes. Chloride transport across the cell membrane is tightly regulated and plays a major role in maintaining the cell volume, the extracellular fluid volume and intracellular pH for instance.

To measure the chloride concentration in body fluids (sweat, blood, urine) can be a first importing step in medical analysis and diagnostics. But to understand the pathomechanisms, it would be desirable to determine the chloride concentration not only in body fluids but also in the cytosol and intracellular compartments.

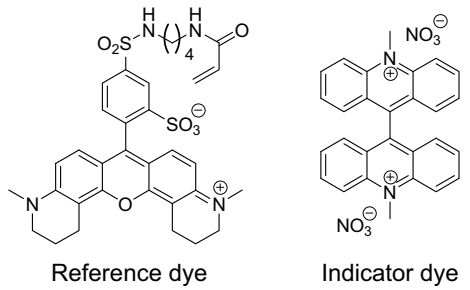

Figure 5. Structures of the dyes used for the preparation of chloride-nanosensors.

In this study we used the acridinium-based dye lucigenin to measure the Cl^- concentration and, as reference dye, we choose the rhodamine-based dye, which has a polymerisable function and can be covalently attached to the polyacrylamide matrix (see Fig5). Polyacrylamide nanoparticles are prepared by inverse microemulsion polymerisation during which both dyes are incorporated. The resulting nanoparticles show a bimodal size distribution in aqueous suspension, consisting of major part with a hydrodynamic diameter of 24 nm and a minor fraction with a diameter of 200 nm (see Fig6a). The resulting broadness of the distribution is indicated by a polydispersity index of 0.32.

The excitation and emission spectra of lucigenin and the rhodamine dye are only slightly changed, when incorporated into the polyacrylamide nanoparticles. The Stern-Volmer constant for quenching of lucigenin by chloride inside the particles was found to be 53 M^{-1} (see Fig6b). This decrease of the quenching rate in the particles compared to the rate in solution (i.e. 250 M^{-1}) can be explained by the immobilization of lucigenin in the polymer matrix. In the polymer, the access to the dye is hindered, which leads to a lower probability of encounters between dye and quencher and thus to smaller quenching constants. Another reason for lower chloride quenching rates might be that a Donnan potential builds up between the polymer and the surrounding media which impedes anions such as chloride from entering into the matrix. Cross-reactivity experiments have shown that, in polymer matrix, quenching by hydroxyl ions dominates over the reduced quenching of chloride thanks to a better diffusion through the hydrophilic matrix, whereas in solution quenching by chloride is by far more effective. Phosphate, which was used in this study as buffer, did not have any significant effect on lucigenin fluorescence in concentrations ranging from 0 to 22 mM. The same applies to sulfate, which was tested in concentrations ranging from 0 to 14 mM sulfate.

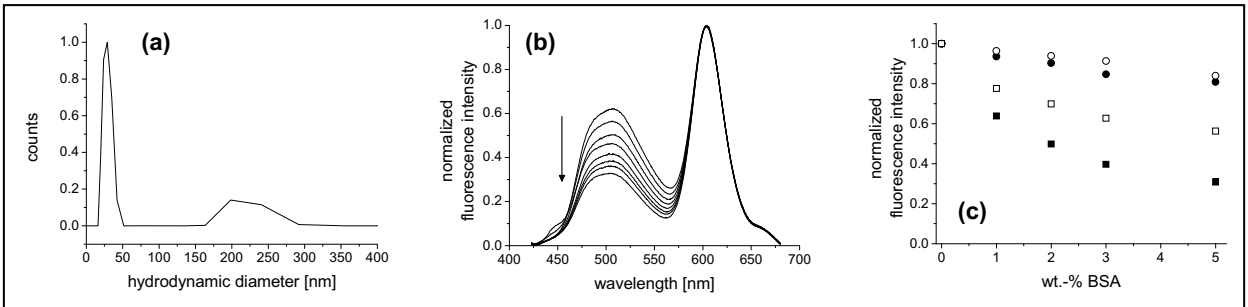

Figure 6. (a) DLS size distribution profile of the chloride-nanosensors ; (b) Fluorescence spectra at different chloride concentration ; (c) Effect of bovine serum albumin (BSA) on fluorescence of lucigenin. Lucigenin (■) and rhodamine **R3** (□) in solution; lucigenin (●) and rhodamine **R3** (○) incorporated into particles. The fluorescence of the solutions and suspensions was excited at a wavelength of 430 nm, to avoid auto-fluorescence of BSA. All spectra were recorded in a phosphate buffer of pH 7.2.

In presence of bovine serum albumin, lucigenin and rhodamine fluorescence are considerably quenched when free in solution while embedded in nanoparticles the fluorescence intensity of the protected dyes

decreases only slightly (see Fig 6c). To test the nanosensors in living cells, we incorporated them into Chinese hamster ovary (CHO) cells and mouse fibroblasts. The nanosensors are distributed in the cytosol leaving the nucleus blank and both dyes are equally distributed in the cytosol. The reference signal is almost constant and, as expected, lucigenin fluorescence decreases at higher Cl^- concentrations and reaches the original value after an exchange of the superfusing solution to the initial Cl^- concentration.

4. Conclusions

Two different types of nanosensors have been successfully prepared that allow the real-time monitoring of pH and chloride based on the incorporation of indicator and reference dyes.
The first one is the 3-hydroxyflavone/fluorescein core-shell nanosensor based on reference dye-doped zeolite *beta* nanoparticles for ratiometric pH measurements. This inorganic nanosensor offers adequate sensitivity, stability and response time in the visible spectral range. The pK_a of 6.4 allows monitoring pH in biological and medical research, e.g. in living cells, tissues and microorganisms. Furthermore, the intrinsic features of the silicate-based nanosensors, i.e. biocompatibility and ease in functionalisation, as well as their nanometric size could make this new nanomaterial suitable for *in vitro* and *in vivo* pH monitoring of relevant biological materials. In addition, other reference dyes may be inserted into zeolite cavities, and the outer surface of the nanodevices may be modified to provide targeting and/or drug delivery functions while simultaneously enabling sensing of e.g. pH.
The second one is an organic polymer nanosensor that allows ratiometric fluorescent measurements of chloride. *In vitro* characterization of the particles shows cross-reactivity to other halide ions, but, because of their low concentrations in biological samples, this effect can be neglected in biological measurements. However, this hydrophilic nanosensor is also sensitive to changes in pH. This might play a role in experiments where intracellular pH changes are observed. Consequently, the pH has to be monitored and taken into account for the determination of the chloride concentration.

References:

1) T. Doussineau, M. Smaïhi, G. J. Mohr: “Two-dye core/shell zeolite nanoparticles: A new tool for ratiometric pH measurements”, *Advanced Functional Materials* **2008**, *19*, 117-122 and references cited therein.
2) G. J. Mohr, Fibre-optic and nanoparticle-based fluorescence sensing using indicator dyes: Pitfalls, self-referencing, application, and future trends, in Standardization and quality assurance in fluorescence measurements I, (Eds. O. S. Wolfbeis, U. Resch-Genger), Springer Series on Fluorescence, **2008**, pp 347-372; ISBN 978-3-540-75206-6.
3) A. Graefe, S. E. Stanca, S. Nietzsche, L. Kubicova, R. Beckert, C. Biskup, G. J. Mohr: “Development and critical evaluation of fluorescent chloride nanosensors”, *Analytical Chemistry* **2008**, *80*, 6526-6531 and references cited therein.